

Supporting Information

for

Tunable Fluorescein-Encapsulated Zeolitic Imidazolate Framework-8 Nanoparticles for Solid-State Lighting

Tao Xiong,^{a†} Yang Zhang,^{a†} Lorenzo Donà,^b Mario Gutiérrez,^a Annika F. Möslein,^a

Arun S. Babal,^a Nader Amin,^c Bartolomeo Civaleri,^b and Jin-Chong Tan^{*,a}

^aMultifunctional Materials & Composites (MMC) Laboratory, Department of Engineering Science, University of Oxford, Parks Road, Oxford OX1 3PJ, U.K.

^bDepartment of Chemistry, NIS and INSTM Reference Centre, University of Turin, via Pietro Giuria 7, Torino 10125, Italy.

^cDepartment of Chemistry, University of Oxford, Mansfield Road, Oxford OX1 3TA, U.K.

†These authors contributed equally to this work

[*jin-chong.tan@eng.ox.ac.uk](mailto:jin-chong.tan@eng.ox.ac.uk)

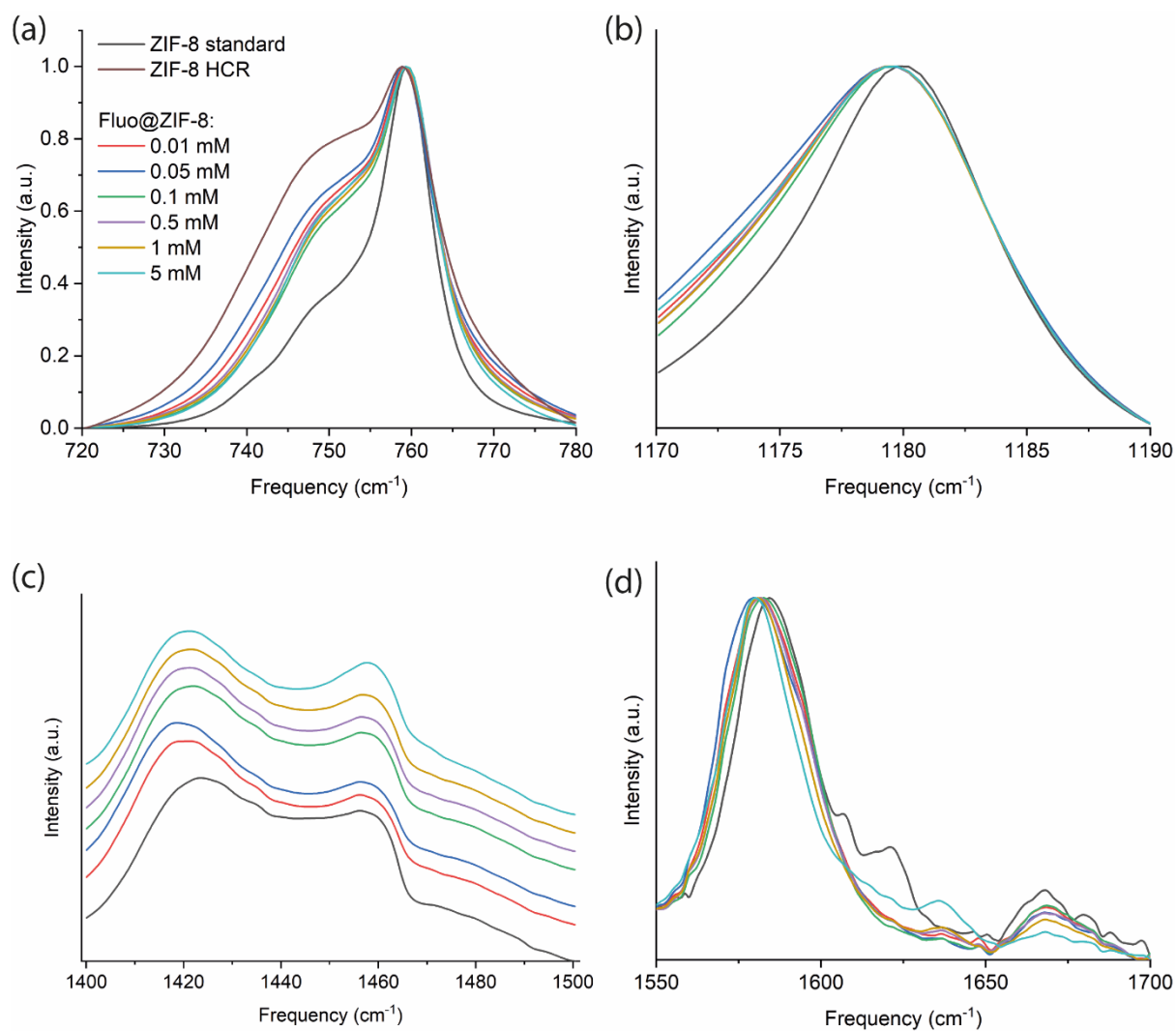


Figure S1. Effects of inclusion of fluorescein guest on the IR spectrum of fluo@ZIF-8. (a) Change of the $749\text{ cm}^{-1} : 759\text{ cm}^{-1}$ peak intensity ratio. (a) Red shift of the 1180 cm^{-1} peak. (b) Red and blue shifts of the 1420 cm^{-1} and 1460 cm^{-1} peaks, respectively. (c) Red shift of the 1584 cm^{-1} peak. Note that the ‘standard’ ZIF-8 sample was obtained using the conventional ‘slow’ synthesis of 24 hours and without the use of Et_3N .

Table S1. Values of lifetime constants (τ_i) and fractional contributions (a_i) of the corresponding emission decay components of the fluo@ZIF-8 samples upon excitation at 362.5 nm, obtained from a multi-exponential fitting function, $I(t) = \sum_i a_i e^{-t/\tau_i}$, where $I(t)$ is the photon counts.

Fluo@ZIF-8 (Fluorescein concentration, mM)	λ/nm	τ_1/ns	a_1/%	τ_2/ns	a_2/%	τ_3/ns	a_3/%
0.01 mM	515			3.9	34.97	6.5	65.03
	525			3.9	17.86	6.5	82.14
	535			3.9	10.45	6.5	89.55
0.05 mM	520			3.9	49.05	6.6	50.95
	530			3.9	30.77	6.6	69.23
	540			3.9	19.31	6.6	80.69
0.1 mM	520	1.1	0.40	3.8	27.70	6.8	71.90
	530	1.1	0.47	3.8	12.60	6.8	86.93
	540	1.1	1.65	3.8	2.58	6.8	95.77
0.5 mM	527	1.1	9.03	3.7	77.24	6.5	13.73
	537	1.1	6.02	3.7	75.98	6.5	18.00
	547	1.1	4.91	3.7	71.98	6.5	23.11
1 mM	529	1.1	41.79	3.0	56.73	6.5	1.48
	539	1.1	36.06	3.0	61.47	6.5	2.47
	549	1.1	33.46	3.0	62.99	6.5	3.55
5 mM	549	0.15	73.63	1.1	20.08	3.4	6.28
	559	0.15	70.12	1.1	22.29	3.4	7.60
	569	0.15	66.39	1.1	23.37	3.4	10.24

Methods for pH response and solvatochromic studies

5 mg of 0.01 mM fluo@ZIF-8 is added to 20 mL of McIlvaine buffer solutions¹ with pH 4, 6, 7, 8, and 10, respectively. The mixture is sonicated before use for excitation and emission measurements.

The sample preparation step for solvatochromism study is very similar, except that buffer solutions are replaced by a variety of solvents, respectively, to form a suspension of the sample after sonication. More specifically, 5 mg of 0.01 mM fluo@ZIF-8 is added to 20 mL of a variety of solvents, respectively, to form the sample suspension.

The excitation and emission spectra of the suspensions in buffer solutions and in solvents, respectively, are measured and compared to that of the solid sample of 0.01 mM fluo@ZIF-8.

pH response of fluorescein@ZIF-8

The spectral response of the 0.01 mM fluo@ZIF-8 sample to pH is investigated (Figure S2). From neutral to basic conditions (pH = 7, 8, 10), the excitation spectra show no significant changes with respect to each other. This reflects the fact that the dianion form is favored at more basic condition. It has been reported that when the pH is below 6.43, the anion form starts to dominate until the pH is below 4.31 when the neutral forms contribute more². At pH = 6, the excitation spectrum already shows a higher contribution at larger excitation energies. At pH = 4, the framework structure of ZIF-8 eventually decomposes³ and the encapsulated fluorescein (in whatever form) is released in the aqueous solution and the spectrum agrees with reported data. At all pH values considered in the experiment, the excitation spectrum is blue-shifted by 0.1 – 0.2 eV. This could be a solvent effect (see the next section on solvatochromism), since water is a polar protic solvent, just like MeOH.

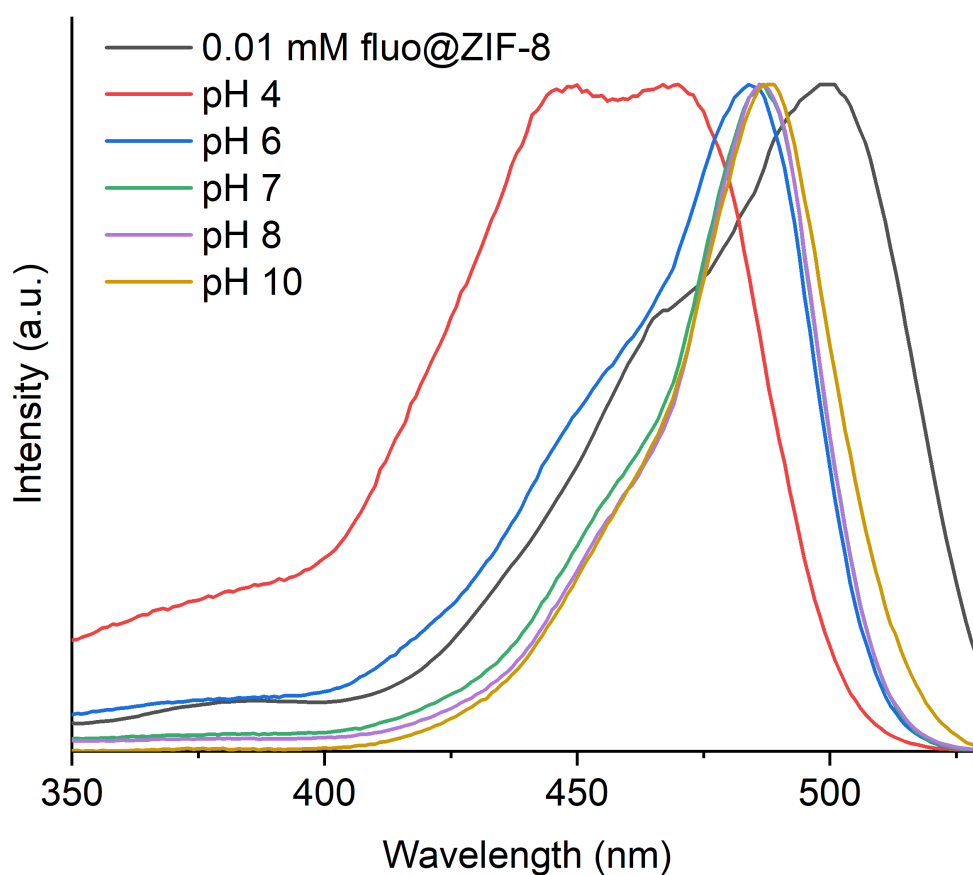


Figure S2. The normalized excitation spectra (observed at emission wavelength 560 nm) of 0.01 mM fluo@ZIF-8 and its suspension in buffer solutions with pH values of 4, 6, 7, 8 and 10, respectively.

Solvatochromism of fluorescein@ZIF-8

The effect of a variety of solvents on the excitation and emission spectra of the lowest concentration sample 0.01 mM fluo@ZIF-8 is studied (Figure S3). It turns out that the excitation wavelength of the suspension of 0.01 mM fluo@ZIF-8 in MeOH is blue-shifted by 0.02 – 0.05 eV for each solvent, with the largest shift occurring for MeOH (9 nm, 0.05 eV). The emission spectra undergo a similar blue shift by 0.05 – 0.06 eV.

An explicit solvation model is utilized to understand this observation (Tables S2-S3). On the one hand, one MeOH solvent molecule is introduced to interact with different functional groups of the carboxylate anion and dianion, respectively. On the other hand, five MeOH solvent molecules are included in the model and they can interact with different functional groups of the fluorescein species simultaneously. Using time-dependent DFT (TDDFT), the vertical excitation energy to the lowest bright state (using a criterion of oscillator strength $f \geq 0.1$) of the isolated fluorescein species (anion or dianion) is compared with each of its solvation model. Generally, while the excitation energy for the solvated dianion is similar to the isolated one, it is increased by up to 0.19 eV for the solvated anion. Combined with the evidence and argument presented in the main manuscript, it can be expected that the MeOH solvent molecules affect the excitation spectrum of fluo@ZIF-8 initially *via* interaction through the window apertures (~ 3.4 Å) of the sodalite cage. Although the kinetic diameter of the MeOH molecule (~ 3.6 Å) is relatively larger than allowed by the windows of ZIF-8 to enter the pores, methanol could still penetrate the narrow apertures of ZIF-8 over time due to lattice dynamics of the flexible framework enabled by gate-opening mechanism.^{4,5} Furthermore, the simulated excitation energy shift exhibits the same trend as the experimental observation. The blue shift (0.02 – 0.05 eV) for the latter is smaller than the solvation model, which is expected because (the experimental) interaction through the window is less effective than (the simulated) direct interaction.

The emission spectra also support the above explanation. The emission wavelength for each polar protic solvent is blue-shifted (due to the fluorescein-solvent interaction) but the extent of shift is not too different (because only the -OH group of the solvent molecule is needed to interact with the fluorescein inside the pores so that the size of the solvent molecule plays a relatively minor role). The CIE chart of the suspension (Figure S3d) shows that although for polar aprotic solvents the pattern is less regular, the color rendering performance of the polar protic solvents are more similar as evidenced from the clustering of their coordinates, consistent with the similar nature of the solvent molecular structure.

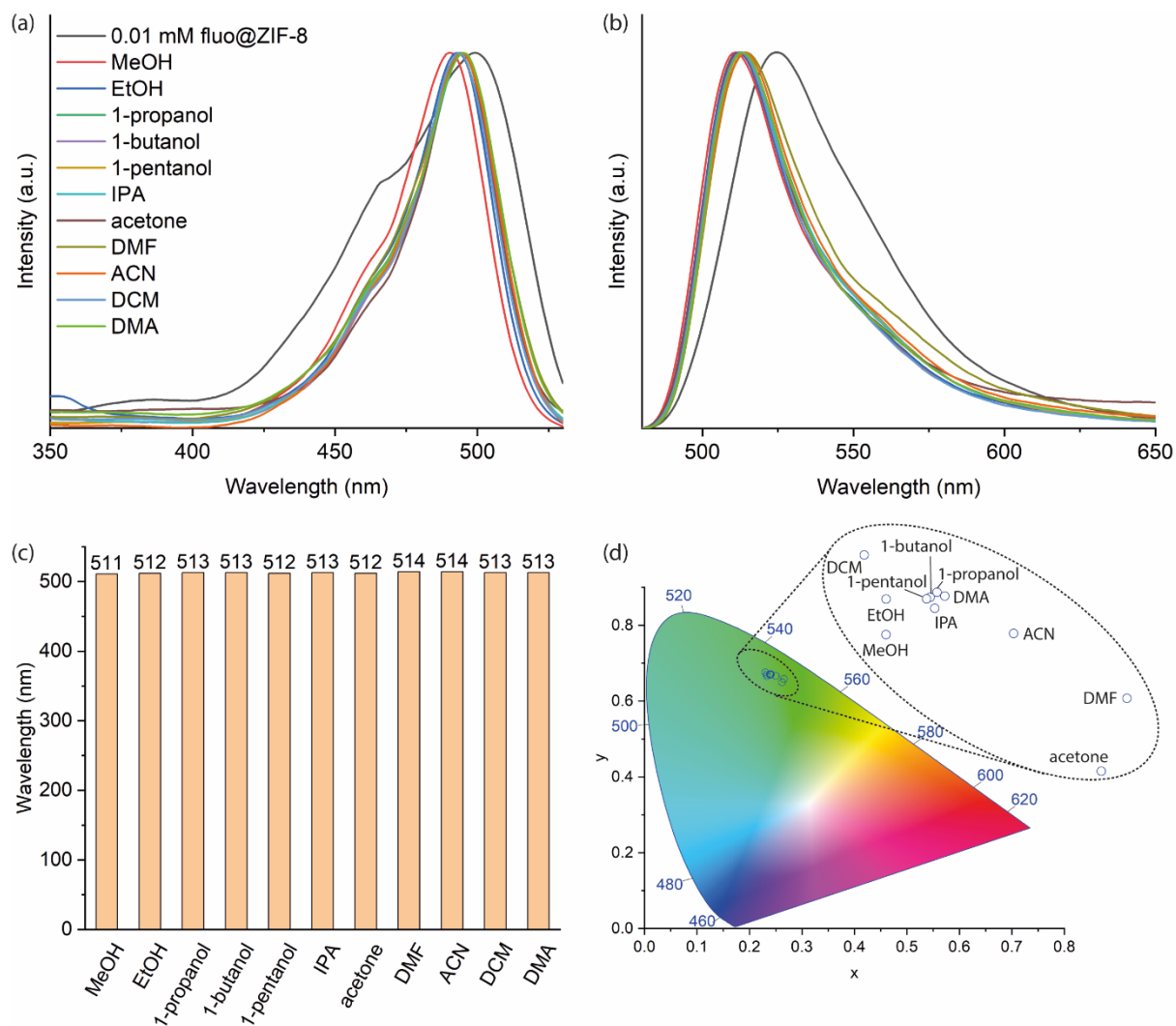


Figure S3. (a) The excitation spectra (observed at emission wavelength 560 nm) of 0.01 mM fluo@ZIF-8 suspension in a variety of solvents. (b) The corresponding emission spectra (excited at 460 nm). (c) The emission maxima in the respective solvents. (d) The CIE 1931 chromaticity diagram of the suspensions.

Table S2. The ground state geometry of fluorescein carboxylate anion in the gas phase (A) and solvated by one MeOH molecule (A1-A3) and five MeOH molecules (A4). The vertical excitation energy ΔE_{vert} refers to the vertical excitation at the respective configuration to the lowest bright excited state with oscillator strength ≥ 0.1 . TDDFT calculations performed at the B3LYP/6-311G* level of theory.

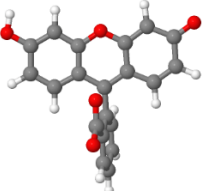
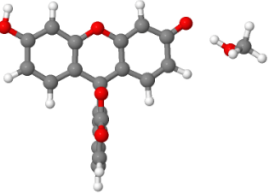
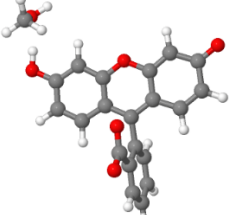
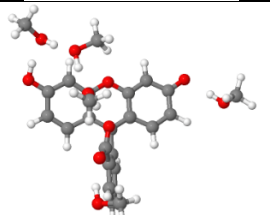
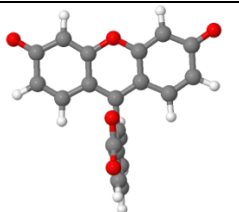
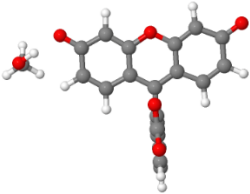
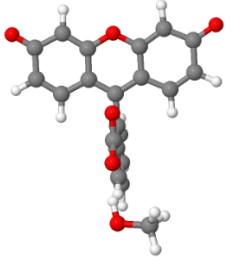
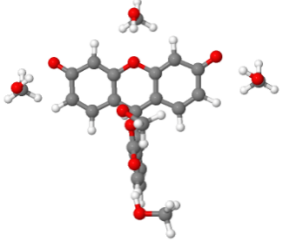
Label	Configuration	ΔE_{vert} (eV)	$\Delta E_{\text{vert}}(\text{solvation}) - \Delta E_{\text{vert}}(\text{gas})$ (eV)
A		2.8732	NA
A1		3.0061	0.1329
A2		2.8735	0.0003
A3		2.9433	0.0701
A4		3.0671	0.1939

Table S3. DFT calculated ground state geometry of fluorescein dianion in the gas phase (D) and solvated by one MeOH molecule (D1, D2) and five MeOH molecules (D3). The vertical excitation energy ΔE_{vert} refers to the vertical excitation at the respective configuration to the lowest bright excited state with oscillator strength ≥ 0.1 . TDDFT calculations performed at the B3LYP/6-311G* level of theory.

Label	Configuration	ΔE_{vert} (eV)	$\Delta E_{\text{vert}}(\text{solvation}) - \Delta E_{\text{vert}}(\text{gas})$ (eV)
D		2.9461	NA
D1		2.9400	-0.0061
D2		2.9561	0.0100
D3		2.9485	0.0024

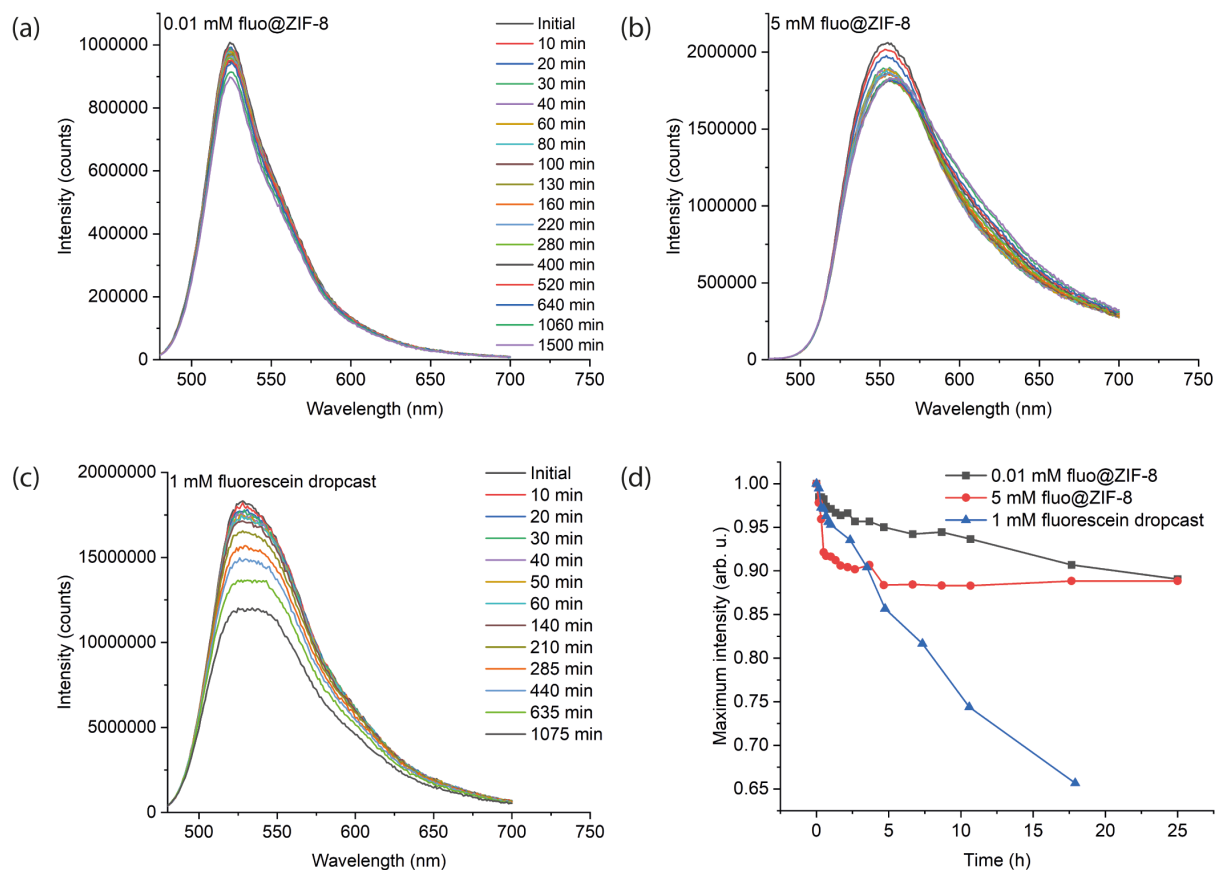


Figure S4. Photostability studies showing the emission spectra of the samples under 450 nm excitation wavelength measured during a prolonged UV exposure time of up to 25 hours. (a) 0.01 mM fluo@ZIF-8. (b) 5 mM fluo@ZIF-8. (c) 1 mM fluorescein in MeOH solution drop casted onto a filter paper. (d) UV-induced photodegradation as a function of exposure time under a Xenon lamp, showing the normalized maximum emission intensity initially set to 1 million counts per second. The lines are guides for the eye.

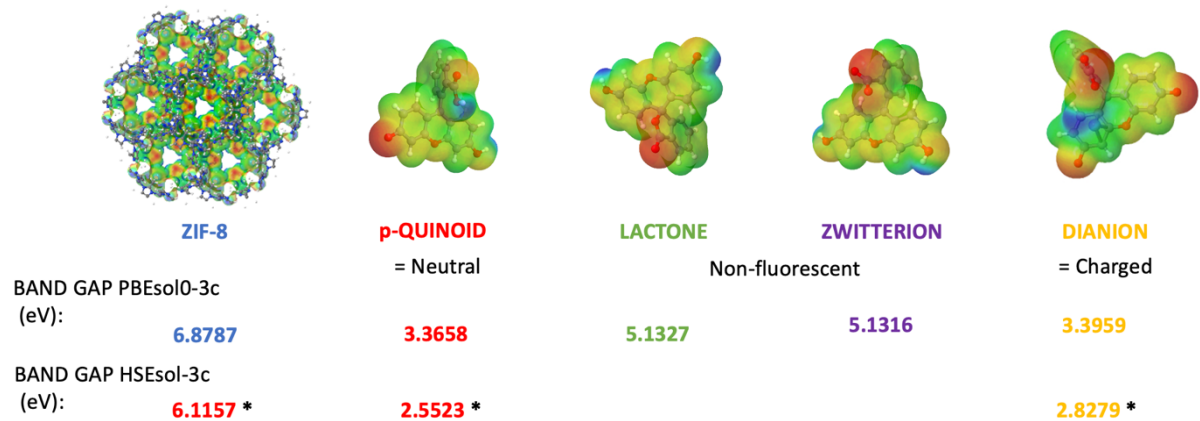


Figure S5. Electrostatic Potential Map (EPM) calculated from CRYSTAL17 code for the ZIF-8 host and the different possible forms of the fluorescein guest. *No geometry optimization performed, band gap obtained from single point energy calculation.

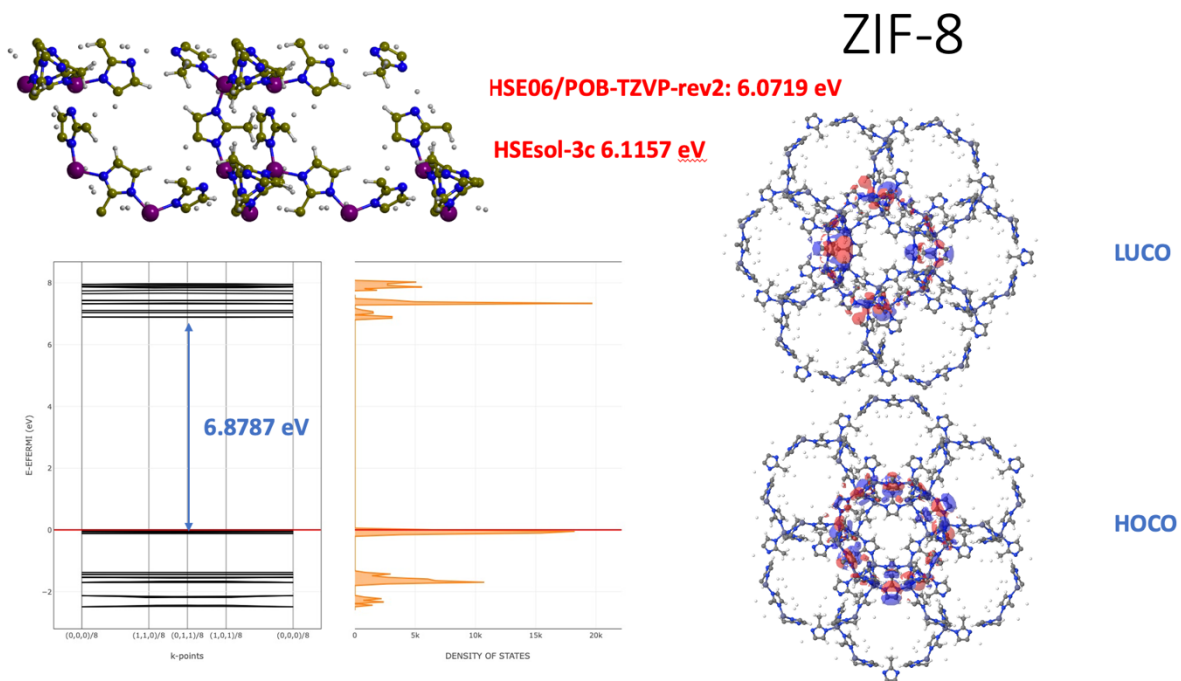


Figure S6. Theoretical calculations of bandgap and LUCO-HOCO crystal orbitals of the porous ZIF-8 framework (host). All periodic DFT calculations employed dispersion interaction using the CRYSTAL17 code. Note the crystal orbitals are localized to the 2-methylimidazolate (mIm) linkers.

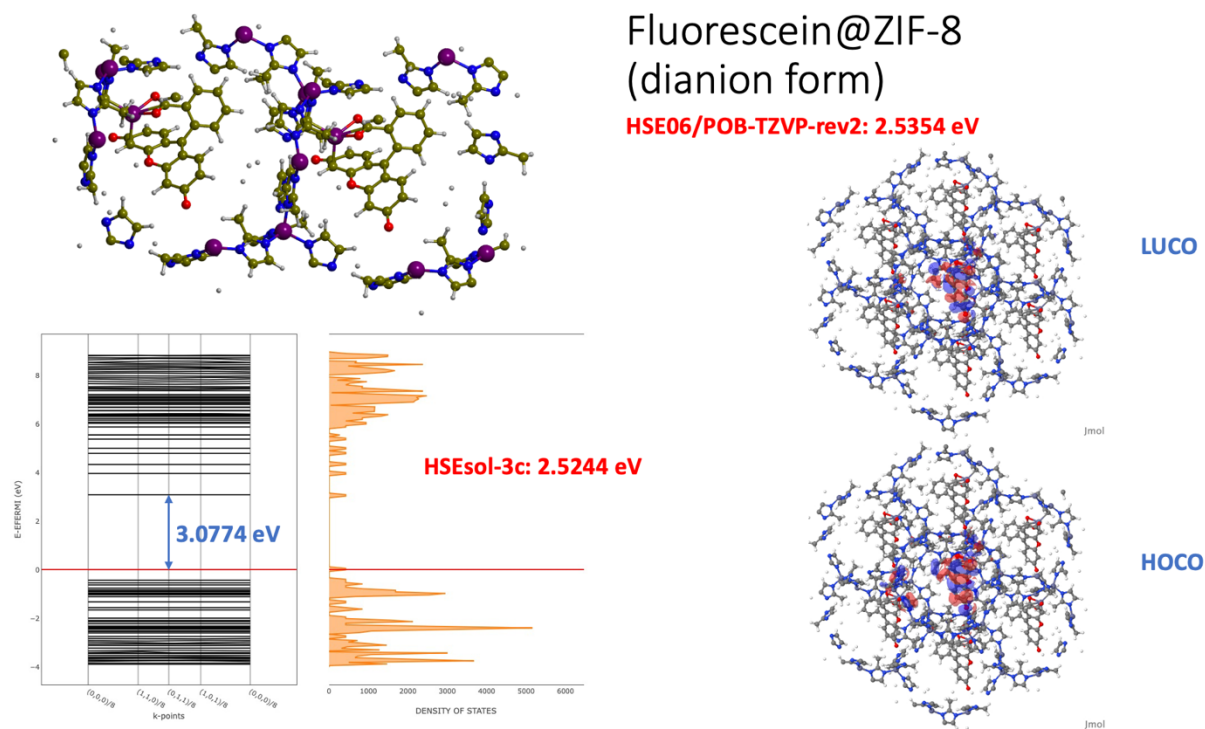
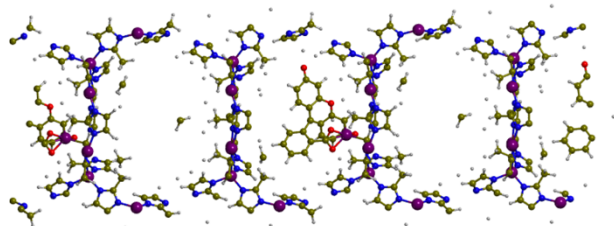


Figure S7. Theoretical DFT calculations of bandgap and LUCO-HOCO crystal orbitals of the fluo@ZIF-8 system. All periodic DFT calculations employed dispersion interaction using the CRYSTAL17 code. Note the crystal orbitals are localized on the fluorescein guest confined in the pore of ZIF-8.

Supercell optimized



Fluorescein@ZIF-8
dianion form:
supercell 2×1×1

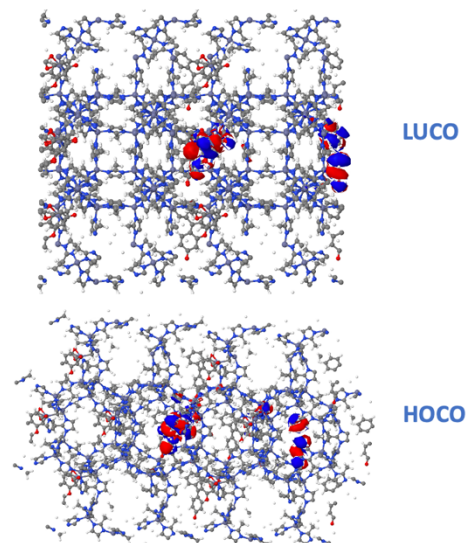
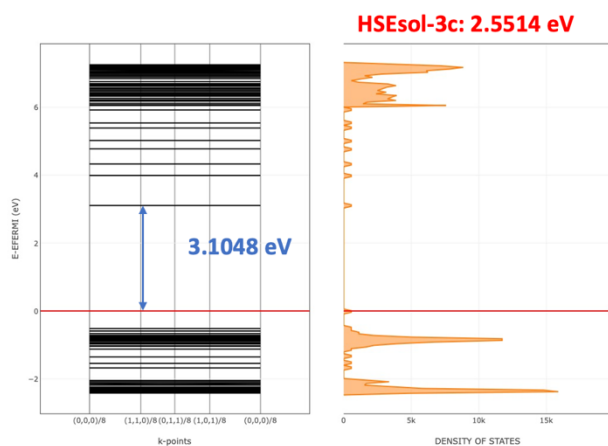


Figure S8. Theoretical DFT calculations of bandgap and LUCO-HOCO crystal orbitals of the 2×1×1 supercell of the fluo@ZIF-8 system. The crystal orbitals are localized on the fluorescein guest molecules confined in the pores of ZIF-8. All periodic DFT calculations employed dispersion interaction using the CRYSTAL17 code.

Table S4. Band gap (in eV) from periodic DFT calculations of the fluorescein dianion@ZIF-8 model system for different loading of the guest molecule confined within the unit cell (of the ZIF-8 host).

Supercell	1×1×1	2×1×1	2×2×1 ^a	2×2×2 ^a
Guest loading	100%	50%	25%	12.5%
PBEsol0-3c	3.077	3.105	3.093	3.090
HSEsol-3c ^b	2.524	2.551	2.539	2.536

^a The geometry of the dianion@ZIF-8 has been fixed at one of the 2×1×1 supercell (see Figure S8)

^b Single-point energy calculations on the PBEsol0-3c optimized geometries.

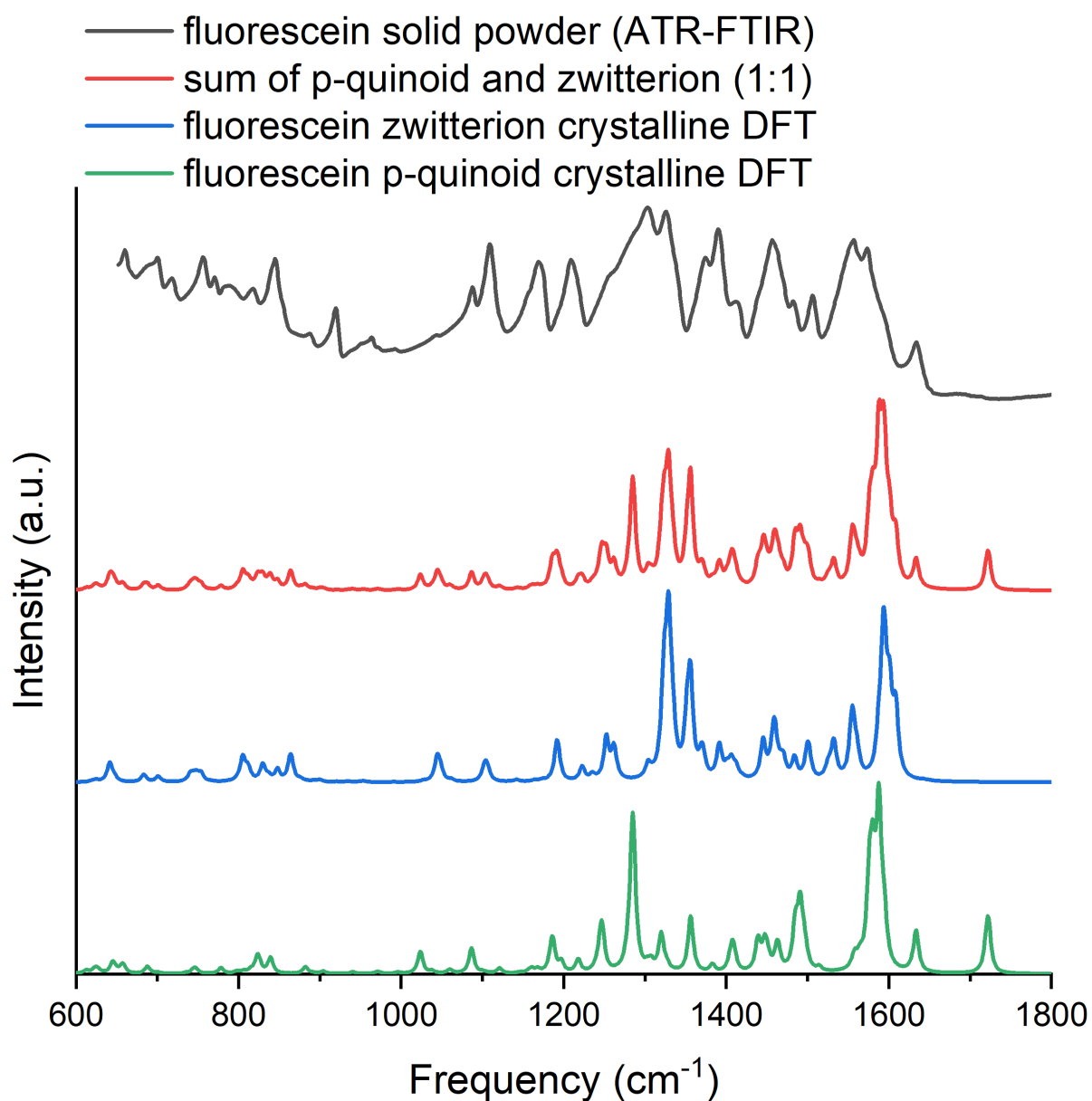


Figure S9. Comparison of the IR spectra of fluorescein solid sample (measured by ATR-FTIR experiment), p-quinoid, zwitterion, and the 1:1 sum of p-quinoid and zwitterion crystalline molecular forms (DFT simulations at PBEsol0-3c level of theory). The simulated spectra have been arbitrarily scaled by a factor of 0.945 for better comparison. A Lorentzian with a FWHM of 10 cm⁻¹ is used to broaden the spectra.

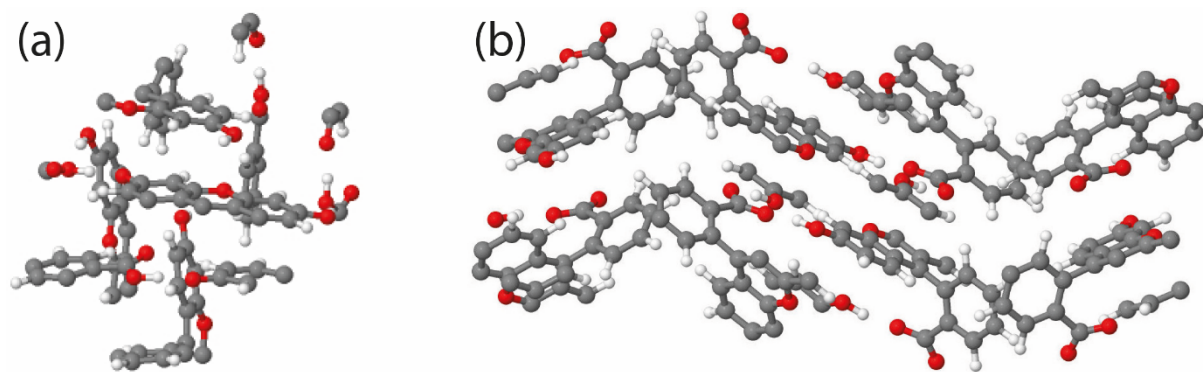


Figure S10. Optimized crystalline structure obtained at the PBEsol0-3c level of theory of fluorescein (a) p-quinoid, and (b) zwitterion.

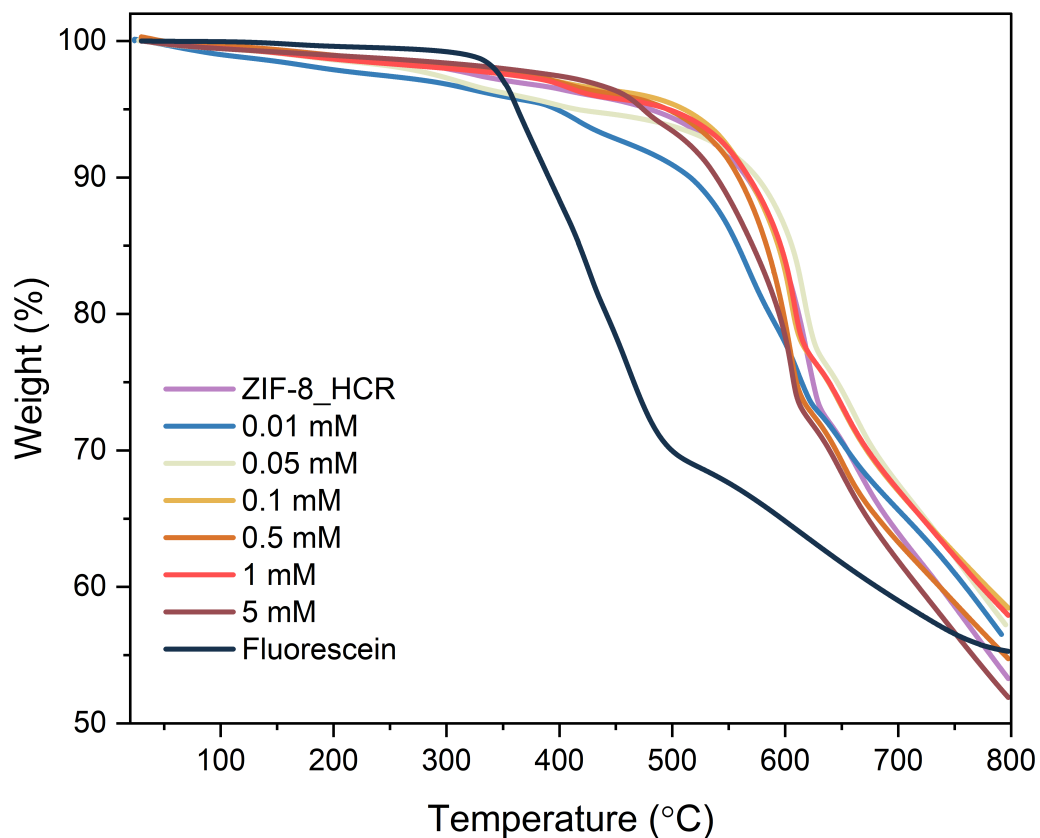


Figure S11. TGA for pristine ZIF-8 (HCR), fluorescein powder, and fluo@ZIF-8 samples. Note the gentle weight loss of ZIF-8 below ~ 300 °C can be attributed to the loss of occluded solvent molecules and Et_3N .

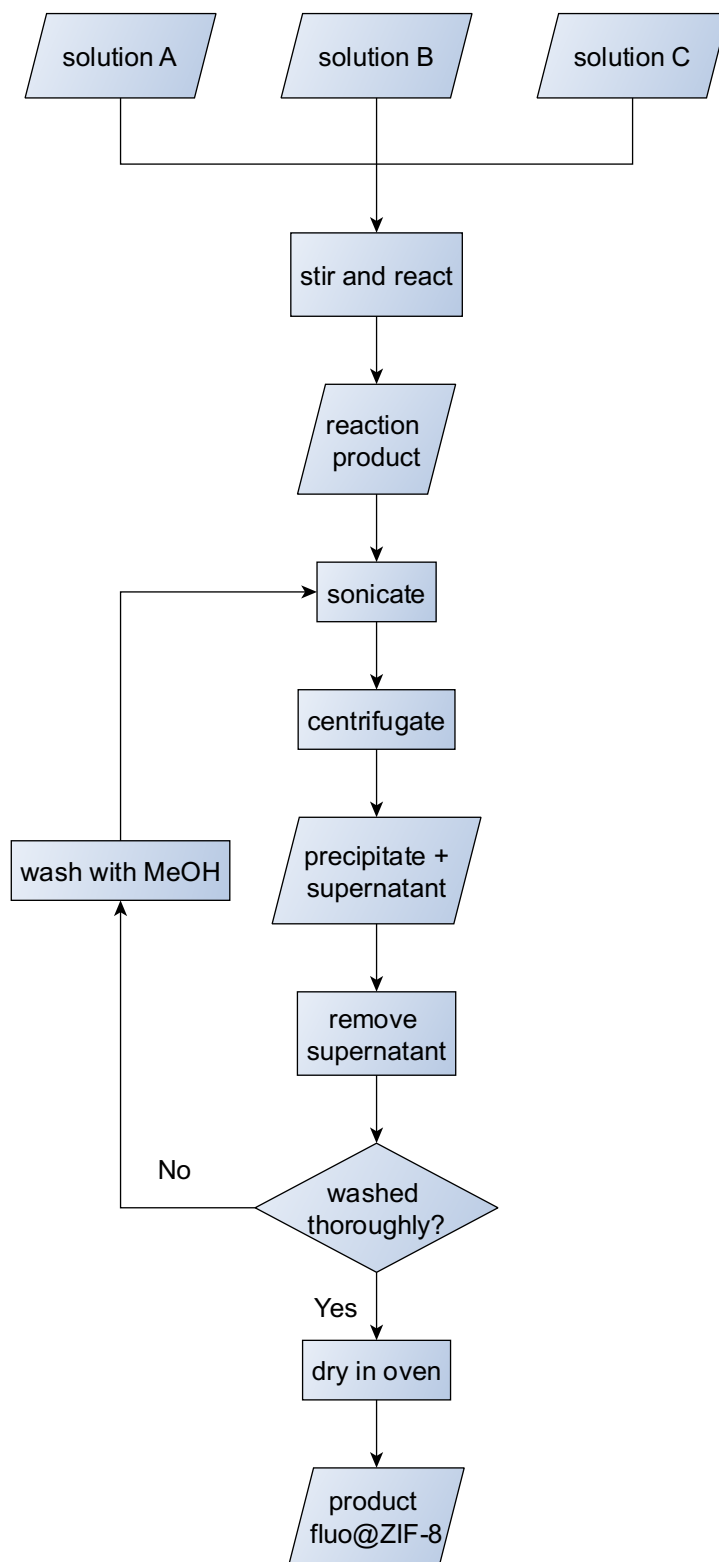


Figure S12. A flowchart of the synthesis of fluo@ZIF-8 samples.

IR spectra of different combinations of solvent and solutes vs fluo@ZIF-8

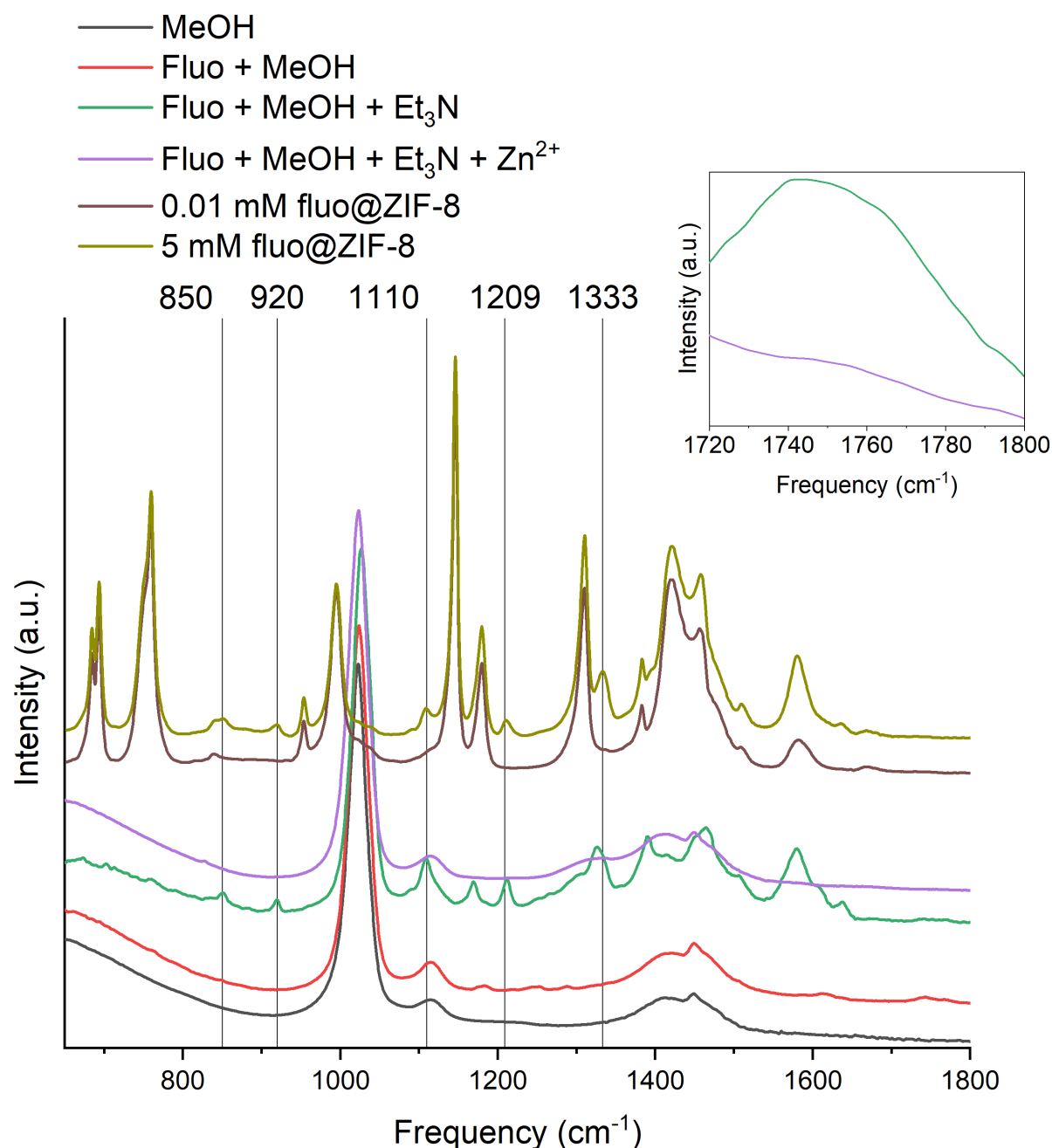


Figure S13. ATR-FTIR spectra for different combinations of solvent (MeOH) and solutes (fluorescein, Et₃N, Zn(NO₃)₂·6H₂O), and selected fluo@ZIF-8 samples.

As *ad hoc* comments in response to reviewer questions, we provide the IR spectra of different combinations of solvent (MeOH) and solutes (fluorescein, Et₃N, Zn(NO₃)₂·6H₂O), and selected fluo@ZIF-8 samples shown in Figure S13. The concentration of fluorescein in MeOH is about 4.7 mM, determined by trial and error so that reasonably strong FTIR signals for fluorescein can be observed. The molar ratio of fluorescein:Et₃N:Zn²⁺ is about 1:15:17.

Note that Et₃N is in excess so that fluorescein is deprotonated. The star-marked peaks in Figure 2 of main manuscript (also marked with vertical lines in Figure S13, i.e. 850, 920, 1110, 1209, and 1333 cm⁻¹) match the deprotonated fluorescein (Fluo + MeOH + Et₃N) peaks very well, justifying the validity of using dianion/anion as the basis of the computation. The inset shows the change of the signal of COO⁻ group in the region of 1750 cm⁻¹, which is a sign that coordination occurred for fluorescein to Zn²⁺. We propose that not all negatively charged fluorescein have Zn²⁺ as counter ions (because the uncoordinated fluorescein seems to fit the experimental data better), but some may be charge balanced by the protonated Et₃NH⁺, the latter case should correspond to the case of the deprotonated fluorescein (Fluo + MeOH + Et₃N). With this interpretation, overall we can still observe the new features in 5 mM fluo@ZIF-8 sample that has highest guest loading.

IR spectra calculated using B3LYP/6-311G* compared with B3LYP/SNSD

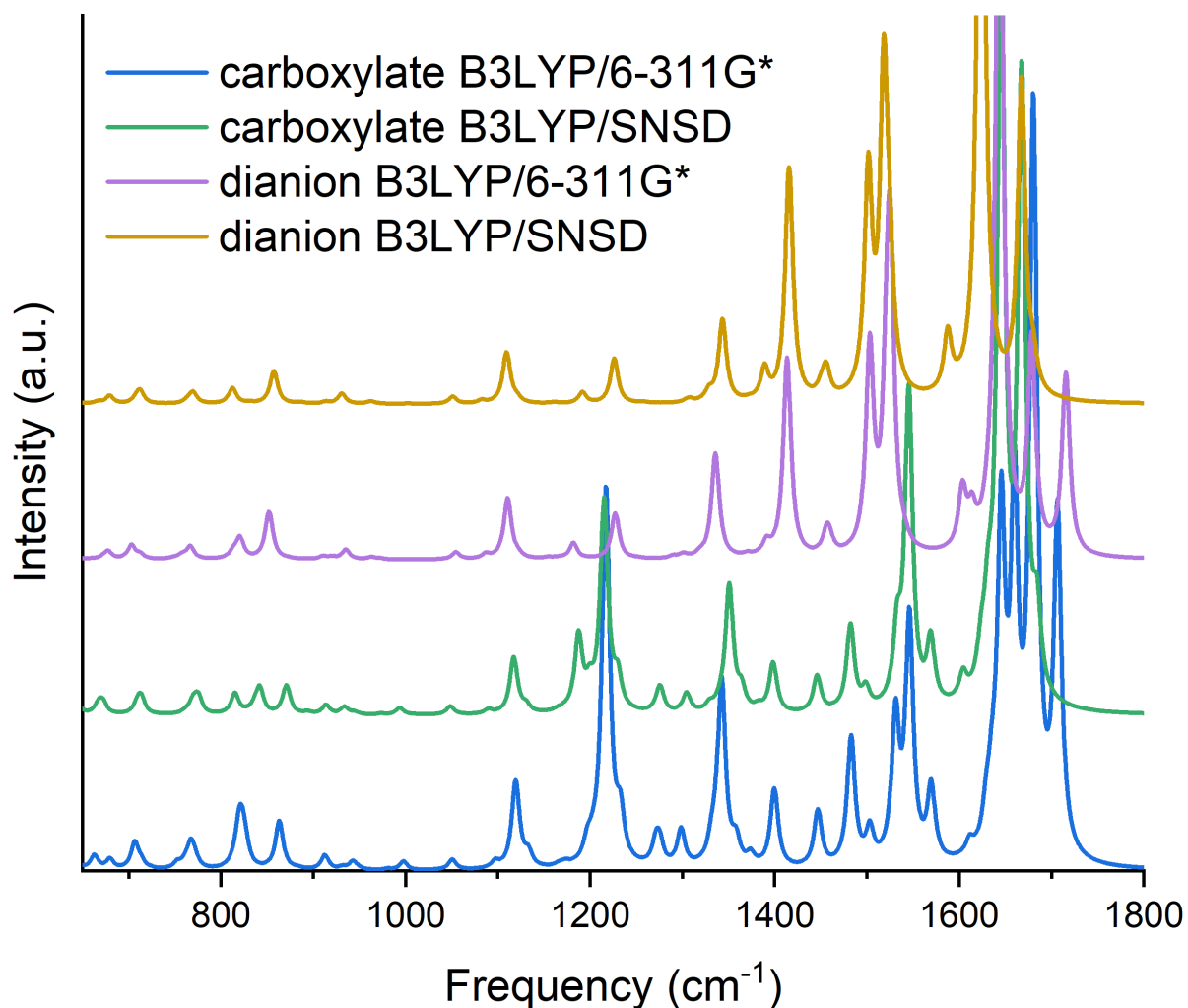


Figure S14. Comparison of IR spectra calculated using B3LYP/6-311G* and B3LYP/SNSD. B3LYP in combination with an improved basis set (SNSD)⁶ for IR predictions to calculate the IR spectra of the anion and dianion. A Lorentzian with a FWHM of 10 cm⁻¹ is used to broaden the spectra. No scaling factor is used. In regions of interest, no significant deviations are found between the two sets of methods.

Solution ^1H NMR spectroscopy of Fluo@ZIF-8

Samples for NMR were dissolved in a solution composed of 500 μL methanol- d_4 and 50 μL $\text{DCl} / \text{D}_2\text{O}$ (35 wt%). All NMR spectroscopy was done at 298 K using a Bruker Avance NEO spectrometer operating at 600 MHz, equipped with a BBO cryoprobe. Data was collected using a relaxation delay of 30 s, with 128k points and a sweep width of 19.8 ppm, giving a digital resolution of 0.18 Hz. Data was processed using Bruker Topspin with a line broadening of 1 Hz and 2 rounds of zero-filling. Peaks were integrated using global spectral deconvolution in the MestReNova software package.

The loading amount, defined as the number of fluorescein molecules per cage (of ZIF-8), was calculated from the molar ratio of fluorescein to 2-methylimidazole (mIm). In order to calculate the molar ratio, peaks corresponding to each compound were integrated and normalised according to the number of protons giving rise to the signal. For fluorescein (fluo), the doublet at approximately 8.30 ppm was used, which corresponds to a single proton (that in the ortho position relative to the carboxyl group). For 2-methylimidazole the singlet at approximately 7.31 ppm was used, which corresponds to the two methine protons of the imidazole ring. Global spectral deconvolution (in the MestReNova software package) was used to pick and integrate the peaks. Each ZIF-8 cage contains 12 methylimidazole ligands. The loading amount was therefore calculated as the molar ratio of fluorescein : methylimidazole multiplied by 12.

Table S5. Guest loading determined from solution ¹H NMR spectroscopy.

Fluo@ZIF-8 (mM used during synthesis)	Molar ratio	Loading of fluorescein (/100%)*
0.01	3649.8	0.00027
0.05	560.5	0.0018
0.1	241.7	0.0041
0.5	53.4	0.019
1	30.0	0.033
5	5.6	0.18

*The loading amount is defined as the number of fluorescein molecules per ZIF-8 cage.

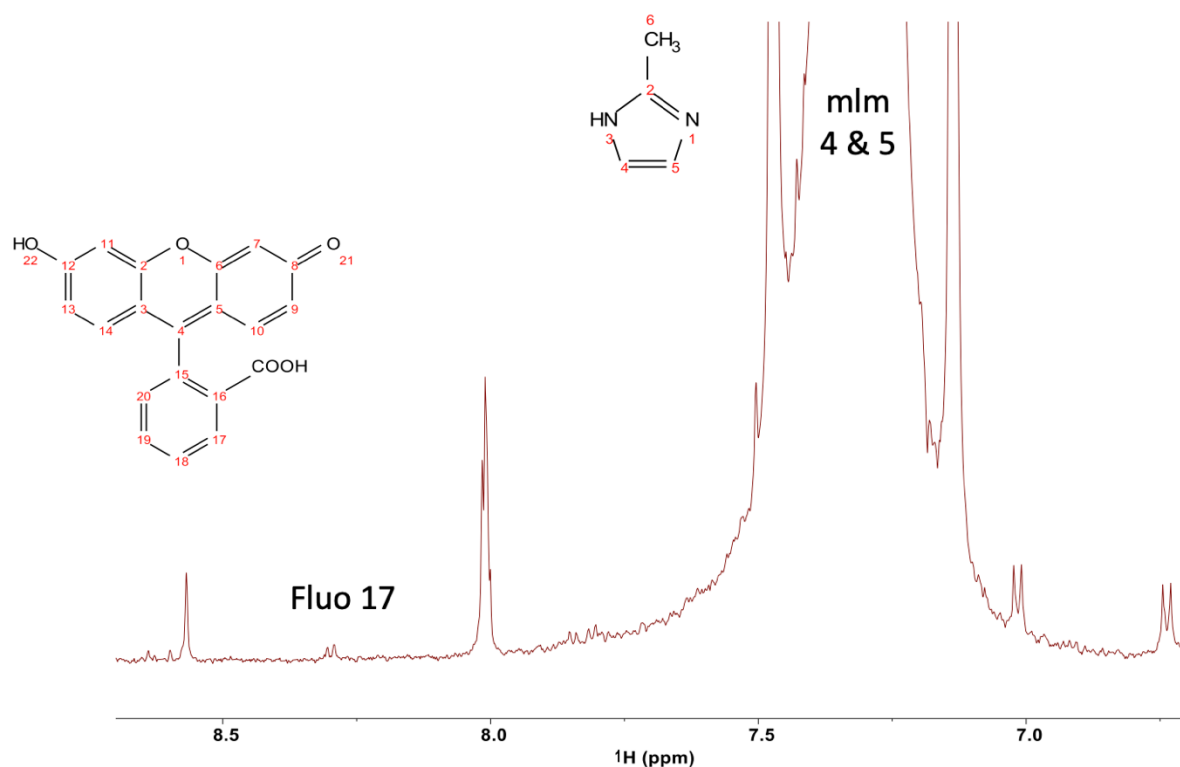


Figure S15. Solution ^1H NMR of 0.01 mM Fluo@ZIF-8 where the guest/host peaks used for integration are indicated as Fluo and mIm, respectively. The guest loading calculated is 1 fluorescein for every 3703.7 cage.

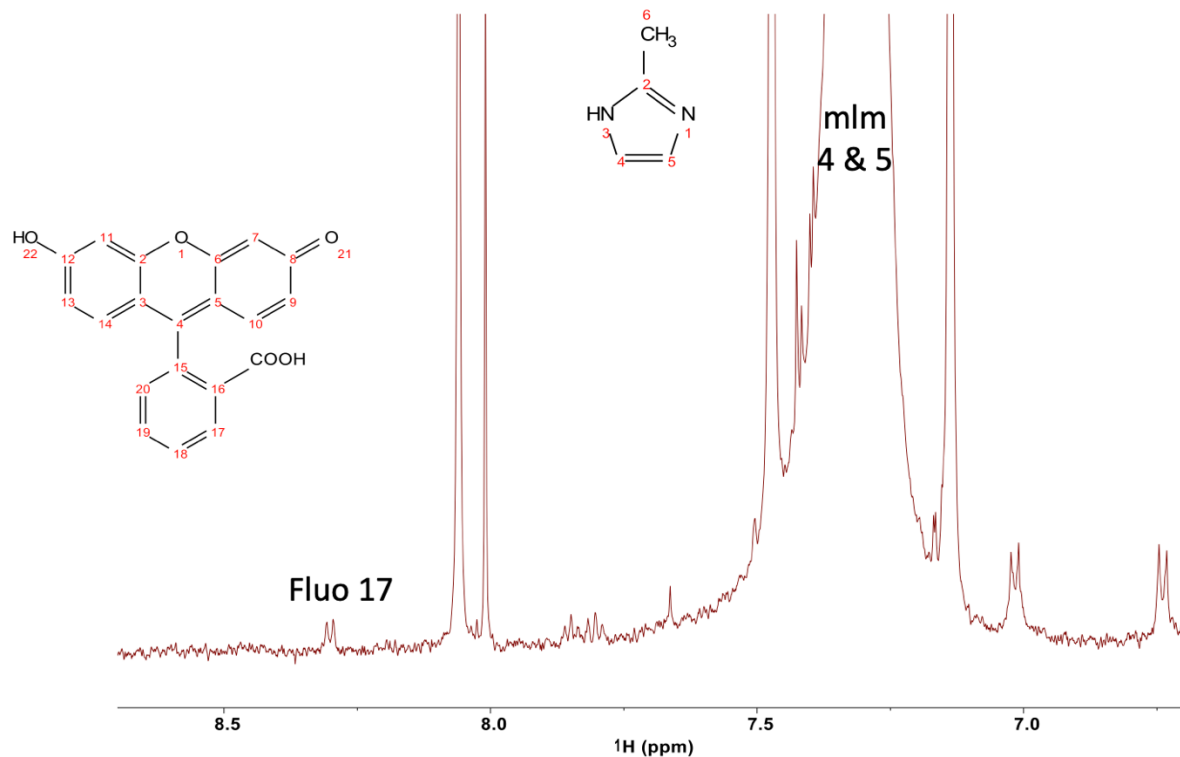


Figure S16. Solution ^1H NMR of 0.05 mM Fluo@ZIF-8 where the guest/host peaks used for integration are indicated as Fluo and mIm, respectively. The guest loading calculated is 1 fluorescein for every 555.6 cage.

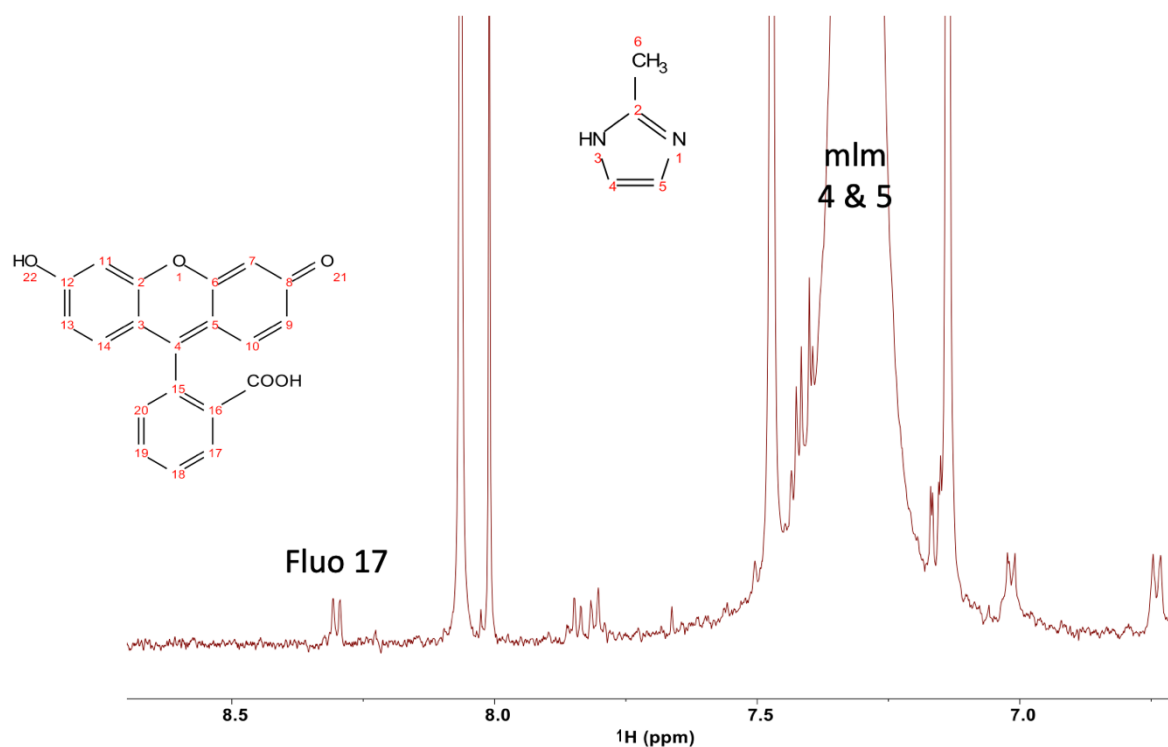


Figure S17. Solution ^1H NMR of 0.1 mM Fluo@ZIF-8 where the guest/host peaks used for integration are indicated as Fluo and mlm, respectively. The guest loading calculated is 1 fluorescein for every 243.9 cage.

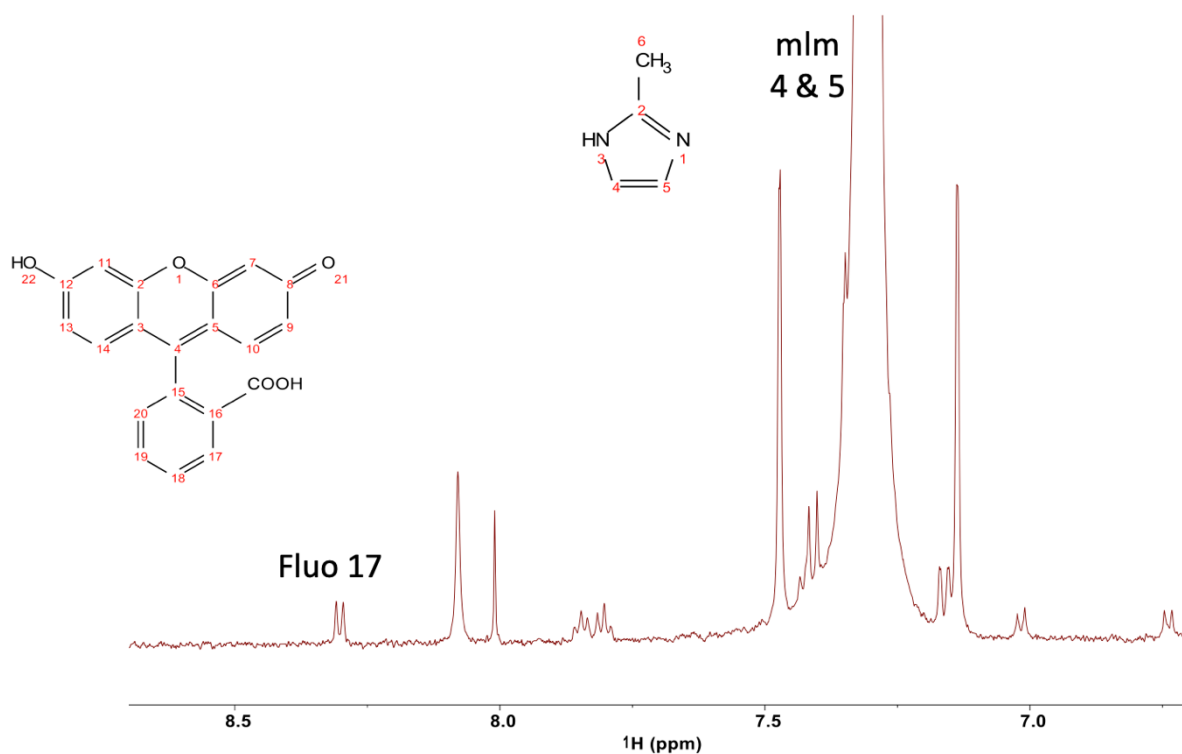


Figure S18. Solution ^1H NMR of 0.5 mM Fluo@ZIF-8 where the guest/host peaks used for integration are indicated as Fluo and mlm, respectively. The guest loading calculated is 1 fluorescein for every 52.6 cage.

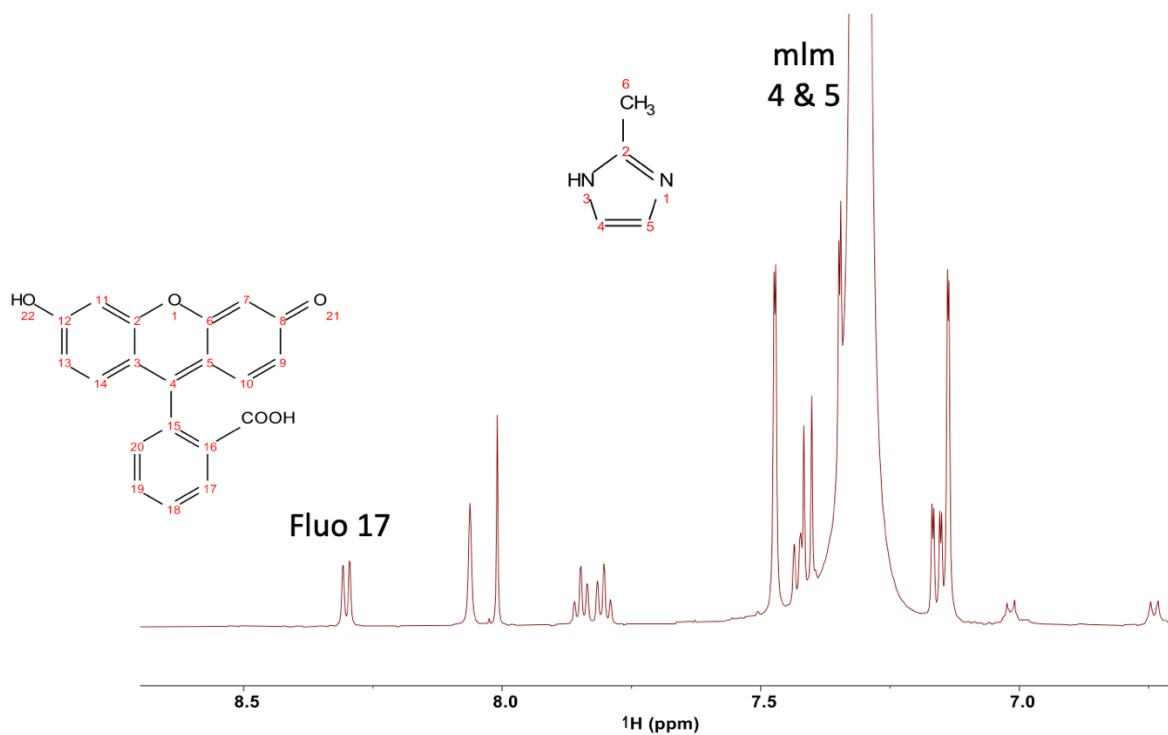


Figure S19. Solution ^1H NMR of 1 mM Fluo@ZIF-8 where the guest/host peaks used for integration are indicated as Fluo and mIm, respectively. The guest loading calculated is 1 fluorescein for every 30.3 cage.

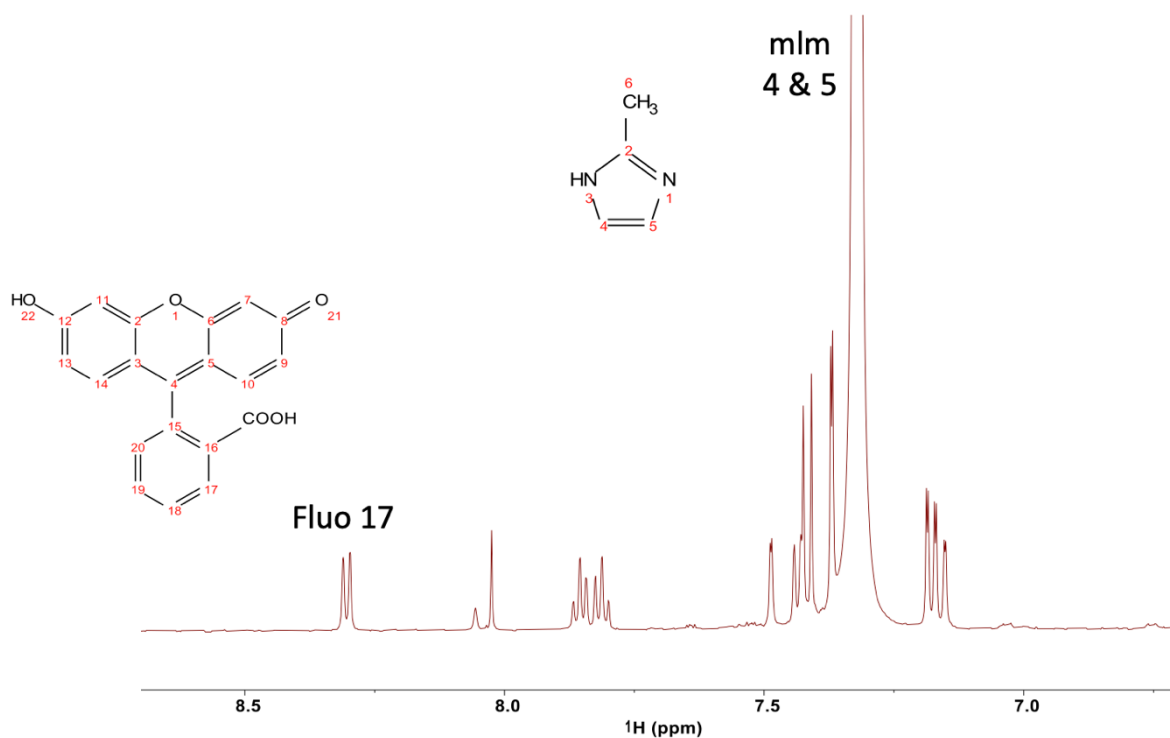


Figure S20. Solution ^1H NMR of 5 mM Fluo@ZIF-8 where the guest/host peaks used for integration are indicated as Fluo and mIm, respectively. The guest loading calculated is 1 fluorescein for every 5.6 cage. Note that it is assumed that all guests are confined in pores even for this high concentration sample.

References

- (1) McIlvaine, T. C. A buffer solution for colorimetric comparison. *J. Bio. Chem.* **1921**, *49*, 183-186.
- (2) Sjöback, R.; Nygren, J.; Kubista, M. Absorption and fluorescence properties of fluorescein. *Spectroc. Acta A* **1995**, *51*, L7-L21.
- (3) Sun, C.-Y.; Qin, C.; Wang, X.-L.; Yang, G.-S.; Shao, K.-Z.; Lan, Y.-Q.; Su, Z.-M.; Huang, P.; Wang, C.-G.; Wang, E.-B. Zeolitic imidazolate framework-8 as efficient pH-sensitive drug delivery vehicle. *Dalton Trans.* **2012**, *41*, 6906-6909.
- (4) Ryder, M. R.; Civalleri, B.; Bennett, T. D.; Henke, S.; Rudić, S.; Cinque, G.; Fernandez-Alonso, F.; Tan, J.-C. Identifying the role of terahertz vibrations in metal-organic frameworks: From gate-opening phenomenon to shear-driven structural destabilization. *Phys. Rev. Lett.* **2014**, *113*, 215502.
- (5) Moggach, S. A.; Bennett, T. D.; Cheetham, A. K. The effect of pressure on ZIF-8: Increasing pore size with pressure and the formation of a high-pressure phase at 1.47 GPa. *Angew. Chem. Int. Ed.* **2009**, *48*, 7087-7089.
- (6) Barone, V.; Ceselin, G.; Fuse, M.; Tasinato, N. Accuracy meets interpretability for computational spectroscopy by means of hybrid and double-hybrid functionals. *Front Chem* **2020**, *8*, 584203.